



The evolution of developmental timing in natural enemy systems

Emily Hackett-Jones^{a,b,*}, Andrew White^c, Christina A. Cobbold^d

^a Department of Mathematics and Statistics, University of Melbourne, Parkville, VIC 3010, Australia

^b School of Mathematics and the Maxwell Institute for Mathematical Sciences, University of Edinburgh, Mayfield Road, Edinburgh EH9 3JZ, UK

^c Department of Mathematics and the Maxwell Institute for Mathematical Sciences, Heriot-Watt University, Edinburgh EH14 4AS, UK

^d Department of Mathematics, University of Glasgow, University Gardens, Glasgow G12 8QW, UK

ARTICLE INFO

Article history:

Received 18 October 2010

Received in revised form

20 December 2010

Accepted 24 December 2010

Available online 30 December 2010

Keywords:

Adaptive dynamics

Host–parasitoid

Phenology

Mathematical model

ABSTRACT

Natural parasitoid systems exhibit considerable variation in their life history properties yet little is known about the effects of development time on parasitoid fitness or of the conditions that might select for rapid development at the expense of reduced parasitoid growth. In this study the techniques of adaptive dynamics are applied to a discrete time host–parasitoid model to examine the evolution of parasitoid life history strategies. In particular, we explore the conditions that select for variation in parasitoid traits, such as, the timing of parasitoid attack and emergence from the host. The process of evolutionary branching, leading to dimorphism, can occur when the benefits to reproduction of early parasitoid attack are bought at a cost in terms of mortality of late parasitoid emergence from the host. We also find that trends in parasitoid life history traits depend critically on the nature of the underlying population dynamics. Increases in the strength of host density-dependence acts to select for shorter parasitoid development time and lower searching efficiency when the underlying population dynamics are at equilibrium. This trend is reversed when the underlying population dynamics exhibit fluctuations. Here, fluctuations in host density driven by parasitism become more extreme as the strength of host density-dependence decreases and so the parasitoid selects early emergence to avoid the mortality experienced at outbreak host densities. Our results are consistent with the general principle that parasitoids facing high mortality risk favour short development times over size and high searching efficiency, whereas species facing low mortality risks favour size at the cost of increased development time.

Crown Copyright © 2011 Published by Elsevier Ltd. All rights reserved.

1. Introduction

Insect parasitoids lay their eggs on or near a host, usually an insect herbivore, and the parasitoid larvae develop by consuming the host tissues. The population dynamics of the host and parasitoid are therefore closely interconnected and parasitoids can act to depress host outbreaks and are important for the control of insect pests (Berryman, 1996). Hosts suffer attack from a range of parasitoid species (Godfray, 1994; Hawkins, 1994; Memmott et al., 1994) and these parasitoids differ considerably in their life history traits. For instance, parasitoids may attack different life stages of the host, the duration of attack may differ (Godfray and Waage, 1991), and the parasitoids may have different attack efficiencies (Parry, 1994). The length of time required to complete development in the host can also vary, leading to different parasitoid emergence times. Since there is such variation in parasitoid life

history properties it is important to understand the conditions that might select for different parasitoid traits. To determine such conditions we outline theoretical techniques to explore the evolution of parasitoid life history parameters, in particular, the evolution of development time and the timing and efficiency of attack. The findings help explain the generation and maintenance of the variation in parasitoid properties observed in natural systems.

Theoretical studies that examine evolution in host–parasitoid systems have chiefly focused on host evolution. These studies investigate how hosts have evolved to evade parasitism through changes to the duration of host development, the use of diapause and host refuges (Kon and Takeuchi, 2001; McGregor and Roitberg, 2000; Ringel et al., 1998; Holt et al., 1999). More recently studies have examined the co-evolution of parasitoid virulence and host resistance, which can be viewed in terms of an arms race between virulence and resistance. When resistance is more costly hosts may select not to invest in resistance, and in spatial models maladaptation becomes possible giving rise to a mismatch between host resistance and parasitoid virulence within a patch (Sasaki and Godfray, 1999; Fellowes and Travis, 2000; Sisterson and Averill, 2004; Gandon et al., 2006). While the study of resistance and virulence has very broad

* Corresponding author at: Department of Mathematics and Statistics, University of Melbourne, Parkville, VIC 3010, Australia.

E-mail addresses: emilyhj@unimelb.edu.au (E. Hackett-Jones), a.r.white@hw.ac.uk (A. White), c.cobbold@maths.gla.ac.uk (C.A. Cobbold).

implications, it does not address the question of how parasitoids may have evolved to successfully locate the host in the first place. One aspect which affects this is related to timing. The duration of the host susceptible period is known to be a determinant for the persistence of the host–parasitoid interaction and it is natural to ask how parasitoid phenology evolves and impacts on persistence.

There are few theoretical studies that focus on investigating parasitoid evolution. An exception is the study by Bonsall et al. (2004) that considers evolution in parasitoid attack rate, competitive ability and parasitoid longevity when the underlying population dynamics are at equilibrium. Parasitoid polymorphism arose when parasitoids had a distinct difference in their life histories (fecundity or longevity) and invading species were found to persist as transients for very long periods. Our study will instead focus on parasitoid phenology, an important consideration given the growing evidence for shifts in insect phenology in many systems (Visser and Both, 2005). We consider the evolution of the parasitoid emergence time, timing of parasitoid attack, and attack rate, and examine how the evolutionary behaviour is modified by constraints between these parameters. We consider the evolution of parasitoid behaviour for both equilibrium and non-equilibrium underlying population dynamics. Stable and unstable dynamics are an important consideration in host–parasitoid models and Holt et al. (1999) had already demonstrated that unstable dynamics can change selective pressures on hosts while White et al. (2006) found large population oscillations can lead to the emergence of polymorphisms.

Modern evolutionary theory (adaptive dynamics) has shown that the feedback between evolutionary and ecological dynamics can lead to disruptive selection, evolutionary branching and therefore to population variation in host–parasite systems (Pugliese, 2002; Dieckmann et al., 2002; Best et al., 2009, 2010). The evolutionary behaviour depends critically on the shape of the trade-off that links evolving life history parameters. We wish to extend the adaptive dynamics techniques to examine the evolution of parasitoid properties. In Hackett-Jones et al. (2009) a framework was developed to represent differences in attack period and emergence time between parasitoids in a host–parasitoid model. The model extends the classical Nicholson–Bailey model (Nicholson and Bailey, 1935) by allowing multiple parasitoids with a full range of possibilities in attack windows and emergence and avoids any implicit hierarchy in parasitoid phenology. This model gives rise to parasitoid coexistence under certain attack–emergence arrangements. This host–parasitoid framework can exhibit equilibrium and non-equilibrium population dynamics (cycles or chaos) and therefore we can examine how variability in population abundance can change the evolutionary behaviour of the parasitoid population. Thus using adaptive dynamics we consider parasitoid evolution within the framework of Hackett-Jones et al. (2009) and explore the conditions under which variation in parasitoid phenology may evolve.

2. The model

We present the generalised discrete-generation host–parasitoid model of Hackett-Jones et al. (2009). The model describes parasitoid phenology (the timing of life history events) in the context of koinobiont parasitoids (these parasitoids allow their host to continue development after parasitism). The model extends the classic Nicholson and Bailey (1935) framework to consider the timing of three parasitoid life history events (described below for two parasitoids P and Q):

1. (t_{ps} or t_{qs}), the time at which adult (P or Q) parasitoids start searching for and parasitising hosts.

2. (t_{pf} or t_{qf}), the time at which adult (P or Q) parasitoids finish searching for and parasitising hosts. The time between starting and finishing searching for hosts is referred to as the *attack window* ($T_p=(t_{pf}-t_{ps})$ or $T_q=(t_{qf}-t_{qs})$).
3. (α_p or α_q), the emergence-time of the (P or Q) parasitoid larvae from a parasitised host relative to the timing of host density-dependent competition. The model assumes parasitised hosts undergo the same competition for resources as unparasitised hosts, therefore a later emerging parasitoid incurs additional mortality via this competition.

Derivation of the model involves solving a system of ordinary differential equations which describe the within season dynamics, as outlined in Appendix A and given in detail in Hackett-Jones et al. (2009). The host suffers attack from multiple parasitoids and these parasitoids will differ in their *attack window*, *emergence time* and *searching efficiency*. In Eqs. (1)–(3) the model framework describes the density in generation n of a single host H_n and two parasitoids, P_n and Q_n . The generalisation to N parasitoids is straightforward.

$$H_{n+1} = e^r e^{-gH_n T_{dd}} H_n e^{-a_p(t_{pf}-t_{ps})P_n} e^{-a_q(t_{qf}-t_{qs})Q_n}, \quad (1)$$

$$P_{n+1} = e^{-gH_n T_{dd} \alpha_p} H_n \left\{ (1 - e^{-a_p(t_2-t_{p(a)})P_n}) + e^{-a_p(t_2-t_{p(a)})P_n - a_q(t_2-t_{q(a)})Q_n} \frac{a_p P_n}{a_p P_n + a_q Q_n} (1 - e^{-(t_1-t_2)(a_p P_n + a_q Q_n)}) + e^{-a_p(t_2-t_{p(a)})P_n - a_q(t_2-t_{q(a)})Q_n} e^{-(t_1-t_2)(a_p P_n + a_q Q_n)} (1 - e^{-a_p P_n (t_{pf}-t_{pb})}) \right\}, \quad (2)$$

$$Q_{n+1} = e^{-gH_n T_{dd} \alpha_q} H_n \left\{ (1 - e^{-a_q(t_2-t_{q(a)})Q_n}) + e^{-a_p(t_2-t_{p(a)})P_n - a_q(t_2-t_{q(a)})Q_n} \frac{a_q Q_n}{a_p P_n + a_q Q_n} (1 - e^{-(t_1-t_2)(a_p P_n + a_q Q_n)}) + e^{-a_p(t_2-t_{p(a)})P_n - a_q(t_2-t_{q(a)})Q_n} e^{-(t_1-t_2)(a_p P_n + a_q Q_n)} (1 - e^{-a_q Q_n (t_{qf}-t_{qb})}) \right\}. \quad (3)$$

The host life cycle is partitioned into attack ‘rounds’ according to the order of parasitoid attack (Fig. 1). We scale time such the host life cycle (egg–adult) takes $T=1$ time units. The terms describing the change in host density between generations (Eq. (1)) have a straightforward interpretation where e^r represents the per capita growth rate of the host in the absence of host density-dependence and the term $e^{-gH_n T_{dd}}$ represents the proportion that survive Ricker type density-dependence over a period T_{dd} time units. The

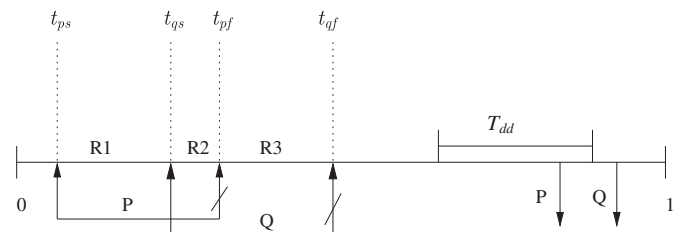


Fig. 1. Illustration of the parasitoid attack and emergence during one host generation. Parasitoid P (Q) commences host attack at time t_{ps} (t_{qs}) and finishes oviposition and searching by time t_{pf} (t_{qf}). The total attack period is divided into ‘rounds’ (R1, R2, etc.) where different numbers of parasitoids attack the host—e.g. in round 1 (R1) only parasitoid P is attacking the host. The emergence time of each parasitoid is indicated by the downward arrows. Host density-dependence operates for a time length T_{dd} during the host generation. Parasitoid P experiences a fraction $\alpha_p < 1$ of the host density-dependence as it emerges before the end of host density-dependence period whereas Q emerges after the density-dependence period and therefore experiences a fraction $\alpha_q = 1$. The ordering of parasitoid attack and emergence and the host density-dependence position and length is only illustrative and the model applies for any combination of these events.

probability that a host escapes parasitism by P is given by the zero term of the Poisson distribution, defined as $e^{-a_p(t_{pf}-t_{ps})P_n}$ where the parameter a_p denotes the searching efficiency of parasitoid P . The probability of a host escaping parasitism by Q is similarly defined as $e^{-a_q(t_{qf}-t_{qs})Q_n}$.

The terms describing the between generation change in parasitoid density also have a straightforward interpretation in terms of the probability that P or Q parasitises the host in a given round of attack. The first term in parentheses in Eq. (2) (i.e. the term $(1-e^{-a_p(t_2-t_{p(a)})P_n})$) is the probability that P parasitises the host in round 1, the second term is the probability that P parasitises the host in round 2 given that neither P nor Q parasitised it in round 1 and the third term is the probability that P parasitises the host in round 3 given that neither P nor Q parasitised it in round 1 or round 2. Hosts parasitised with parasitoid P may also suffer mortality due to the Ricker density-dependence experienced by all hosts meaning that only a proportion $e^{-gH_n T_{dd} \alpha_p}$ survive to become parasitoids where α_p is the fraction of the host density-dependent period experienced by P parasitised hosts. The terms representing the change in density between generations for parasitoid Q (Eq. (3)) can be defined in an analogous manner. Note that the equations apply for any combination of P - Q attack since the ordering determines the parameters $t_1, t_2, t_{p(a)}, t_{p(b)}, t_{q(a)}, t_{q(b)}$ which act to turn on or off particular rounds. In our model parasitoids do not compete directly for hosts and this allows us to focus on the evolution of phenology. Definitions of model parameters are presented in Table 1, and given together with baseline values.

In the absence of parasitoid (Q_n) the model collapses to

$$H_{n+1} = e^r H_n e^{-gH_n T_{dd}} e^{-a_p(t_{pf}-t_{ps})P_n}, \quad (4)$$

$$P_{n+1} = H_n e^{-gH_n T_{dd} \alpha_p} (1 - e^{-a_p(t_{pf}-t_{ps})P_n}), \quad (5)$$

Table 1

Definitions of attack window timings and other parameters used in the model. The appropriate baseline values or range of values (in square brackets) are indicated. Note, we present the full parameter definitions in this table to allow the model to be applied to all realistic parameter sets (however, for the baseline parameters used in this study some of the attack window timing definitions could be simplified).

Parameter	Description	Baseline value
t_{ps} (or t_{qs})	Time P (or Q) starts attacking and searching for hosts	[0,0.25]
t_{pf} (or t_{qf})	Time P (or Q) finishes attacking hosts	[0.25,0.5]
$T_p = t_{pf} - t_{ps}$ (or T_q)	Length of P (or Q) attack window	0.25
$t_1 = \min(t_{qf}, t_{pf})$	Time of the first parasitoid to finish attacking	
$t_2 = \min(t_1, \max(t_{ps}, t_{qs}))$	t_2 determines which happens first: a parasitoid has finished attacking (t_1) or both parasitoids have started attacking by $\max(t_{ps}, t_{qs})$	
$t_{p(a)} = \min(t_{ps}, t_1)$	Time P starts attacking or time Q finishes if that happens earlier	
$t_{q(a)} = \min(t_{qs}, t_1)$	Time Q starts attacking or time P finishes if that happens earlier	
$t_{p(b)} = \max(t_{ps}, t_1)$	Time P starts attacking or time Q finishes if that happens later	
$t_{q(b)} = \max(t_{qs}, t_1)$	Time Q starts attacking or time P finishes if that happens later	
T_{dd}	Length of host density-dependent (HDD) period	0.5
g	Strength of density-dependence	1
e^r	Per capita growth rate of hosts	e^1
α_p or α_q	Fraction of HDD experienced by P (or Q)	[0,1]
a_p or a_q	Searching efficiency of P (or Q)	[3,20]

which is discussed in Cobbold et al. (2009). It shows a range of dynamics from stable coexistence of the host and parasitoid to population cycles and chaos. Increases in the emergence-time α_p , stabilise the host–parasitoid dynamics. When $\alpha_p = 0$ we have the classic host–parasitoid model of Beddington et al. (1975), in which host density-dependence is followed parasitism. In the case $\alpha_p = 1$ we recover the model by Wang and Gutierrez (1980) in which parasitism follows host density-dependence. The attack window in these models has the same effect as parasitoid searching efficiency. Thus, increasing the duration of the attack window can destabilise the host–parasitoid dynamics.

2.1. Evolutionary methods for stable point population equilibria

The theory of adaptive dynamics is used to determine the evolution of the parasitoid life history properties in our model. This theory analyses the fitness of a mutant parasitoid, which we assume to be parasitoid Q , attempting to invade an environment composed of a resident parasitoid, P , and a resident host, H . The fitness, denoted $s_P(Q)$, corresponds to the per capita growth rate for Q , or equivalently the largest Lyapunov exponent and is given by Metz et al. (1992) and for our systems is defined as

$$s_P(Q) = \ln(M), \quad \text{where } M = \left. \frac{\partial Q_{n+1}}{\partial Q_n} \right|_{Q_n=0, H_n=H, P_n=P}. \quad (6)$$

Here, H and P are the equilibrium values of the resident host and parasitoid. The fitness can be written explicitly as

$$s_P(Q) = \ln \left\{ e^{-gHT_{dd} \alpha_q} H(a_q(t_2 - t_{q(a)}) + a_q(t_{qf} - t_{q(b)}) e^{-a_p P(t_1 - t_{p(a)})} + \frac{a_q}{a_p P} e^{-a_p P(t_2 - t_{p(a)})} (1 - e^{-a_p P(t_1 - t_2)})) \right\}. \quad (7)$$

Note, the fitness depends on parameters associated with the mutant parasitoid and on the densities of the resident host and parasitoid, H and P (which depend on resident parameters). The unique stable point equilibrium values H and P can be found numerically by solving the following system of equations:

$$P = H(1 - e^{-a_p(t_{pf}-t_{ps})}) e^{-gHT_{dd} \alpha_p}, \quad (8)$$

$$gT_{dd}H = r - a_p(t_{pf} - t_{ps})P. \quad (9)$$

Since P is at its demographic attractor it implies that $s_P(P) = 0$ and this allows us to rewrite the fitness expression (Eq. (7)) as

$$s_P(Q) = \ln(e^{-gHT_{dd}(\alpha_q - \alpha_p)} \Phi), \quad (10)$$

where

$$\Phi = \frac{1}{a_p(1 - e^{-a_p(t_{pf}-t_{ps})})} \{ a_q a_p P(t_2 - t_{q(a)}) + a_q a_p P(t_{qf} - t_{q(b)}) e^{-a_p P(t_1 - t_{p(a)})} + a_q e^{-a_p P(t_2 - t_{p(a)})} (1 - e^{-a_p P(t_1 - t_2)}) \}. \quad (11)$$

This expression proves useful to understand the outcome of parasitoid evolution. The success of the mutant parasitoid can be determined by analysing the fitness function. If fitness is positive the mutant can invade. The population will evolve in small steps in the direction of the local fitness gradient until the fitness gradient is zero where it reaches a singular strategy, v^* , which is a solution of the following expression:

$$\left. \frac{\partial s_P(Q)}{\partial v_q} \right|_{v_q = v_p = v^*} = 0.$$

Here v^* represents the evolving parameter (and in this study we allow at least one of a, α or t_s to evolve). The evolutionary behaviour at the singular strategy is determined by the second derivatives of the fitness function evaluated at the singularity

(Metz et al., 1996; Geritz et al., 1998). The singular point may be evolutionary stable (ES) and convergent stable (CS) in which case it is an uninvadable, evolutionary attractor. If it is neither ES nor CS it is an invadable, evolutionary repeller. If it is ES but not CS it is known as a Garden of Eden strategy (Nowak, 1990) (here the singular strategy is uninvadable but nearby strategies are repelled). The process of evolutionary branching occurs when the singular strategy is CS but not ES. Here we are attracted towards the singular strategy but when nearby it is invadable and disruptive selections leads to dimorphisms.

2.2. Evolutionary methods for periodic, quasiperiodic and chaotic attractors

It is rarely possible to determine the largest Lyapunov exponent (fitness) algebraically when the underlying dynamics are not at a stable point equilibrium (but see Hoyle et al., in press). It is possible, however, to compute the largest Lyapunov exponent numerically (Eckmann and Ruelle, 1985; Metz et al., 1992; Ferriere and Gatto, 1993) under non-equilibrium conditions and the fitness of the mutant strategy Q can be determined by calculating

$$s_P(Q) = \lim_{t \rightarrow \infty} \frac{1}{t} \ln(M_{t-1} \cdot M_{t-2} \cdot \dots \cdot M_1 \cdot M_0), \quad (12)$$

where

$$M_t = \left\{ e^{-gH_t T_{dd} \alpha_q} H_t (a_q(t_2 - t_{q(a)}) + a_q(t_{qf} - t_{q(b)})) e^{-a_p P_t (t_1 - t_{p(a)})} + \frac{a_q}{a_p P_t} e^{-a_p P_t (t_2 - t_{p(a)})} (1 - e^{-a_p P_t (t_1 - t_2)}) \right\}. \quad (13)$$

Here, H_t and P_t are successive population values of H and P for the resident population on its attractor. In practice we numerically determine the value of $s_P(Q)$ in Eq. (12) over a sufficiently long time series (or the cycle period in the case of periodic attractors). The values of $s_P(Q)$ for different resident–mutant combinations can be used to determine the sign structure of the fitness expression and to construct pairwise invadability plots (PIPs) (Metz et al., 1992; Geritz et al., 1998), which can be used to infer the position of the singular strategies and their evolutionary behaviour.

This evolutionary behaviour can be verified by undertaking related multi-strain simulations that represent the adaptive dynamic process. In these simulations, the population dynamics are numerically solved for a fixed time (t_a) according to Eqs. (4)–(5) initially with a monomorphic population. Mutant strains are generated by small deviations around the current evolving parameter v (the choice of current strain from which to mutate depends on its relative density) and introduced at low density. The population dynamics are then solved using Eqs. (1)–(3) (and its multi-strain extensions) for a further time t_a . Strains whose population density falls below a (low) threshold are considered extinct and removed before considering new mutations and repeating the procedure. In this way, the parasitoid parameters can evolve. One difference between the theory and simulations is that the simulations are not mutation-limited (i.e. new mutants could evolve before previous mutants had reached equilibrium or gone extinct). Although this could be overcome by increasing t_a , this set-up has been shown to correctly approximate the evolutionary behaviour predicted by adaptive dynamics in studies where the dynamical attractor is an equilibrium point and has been used successfully to assess the adaptive dynamics for non-equilibrium attractors (White et al., 2006; Hoyle et al., in press).

3. Results

3.1. Evolution of a single parasitoid parameter

When the underlying population dynamics exhibit a stable point equilibrium we can classify the singular strategy analytically. In the case where the attack windows for P and Q are identical Eqs. (10) and (11) can be simplified and the fitness expression becomes

$$s_P(Q) = \ln \left(\frac{a_q}{a_p} e^{-gH T_{dd} (\alpha_q - \alpha_p)} \right). \quad (14)$$

Clearly if $a_p = a_q$ then the fitness is positive when $\alpha_q < \alpha_p$. Similarly, if $\alpha_p = \alpha_q$ the fitness is positive when $a_q > a_p$. Therefore if these life history properties evolve independently, selection will lead to parasitoids that emerge from the host early to minimise the fraction of the host density-dependence phase that they experience (corresponding to a decrease in parasitoid mortality), or that maximise the searching efficiency (corresponding to increased parasitoid fecundity). In the case where the attack windows are the same and the underlying dynamics are non-equilibrium the fitness expressions (using Eq. (12)) can be written as

$$s_P(Q) = \lim_{t \rightarrow \infty} \frac{1}{t} \ln \left(\frac{a_q}{a_p} e^{-gH_{t-1} T_{dd} (\alpha_q - \alpha_p)} \cdot \dots \cdot \frac{a_q}{a_p} e^{-gH_0 T_{dd} (\alpha_q - \alpha_p)} \right). \quad (15)$$

When $\alpha_q = \alpha_p$ in Eq. (15)

$$s_P(Q) = \lim_{t \rightarrow \infty} \frac{1}{t} \ln \left(\frac{a_q}{a_p} \right)^t = \ln \left(\frac{a_q}{a_p} \right) \quad (16)$$

and when $a_q = a_p$ in Eq. (15)

$$s_P(Q) = \lim_{t \rightarrow \infty} \frac{1}{t} \ln (e^{-gH_{t-1} T_{dd} (\alpha_q - \alpha_p)} \cdot \dots \cdot e^{-gH_0 T_{dd} (\alpha_q - \alpha_p)}) \\ = -g T_{dd} (\alpha_q - \alpha_p) \left(\lim_{t \rightarrow \infty} \frac{1}{t} (H_{t-1} + \dots + H_0) \right). \quad (17)$$

Therefore the results for non-equilibrium underlying dynamics are equivalent to those with equilibrium underlying dynamics when the parameter a or α can evolve independently.

Analysis can also be undertaken to assess the evolution of the attack timing (for brevity the analysis is not shown here). If the start of the attack window, t_s evolves independently it can be shown that selection will lead to parasitoids that start their attack earlier (provided the overall attack window is not reduced). This result applies under equilibrium and non-equilibrium population dynamics.

3.2. Evolution of two parasitoid parameters linked by a trade-off

We now consider the evolution of two parasitoid life history parameters. These parameters are linked by a trade-off that ensures that a benefit from a change in one parameter is bought at a cost through a change in the other parameter.

3.2.1. An a versus α trade-off

We consider a trade-off linking α , the parasitoid's emergence time, to a , its searching efficiency (so $a = f(\alpha)$). To ensure the correct cost-benefit structure we impose the constraint that $f'(\alpha) > 0$ representing the situation where an early emerging parasitoid (low α) will be less efficient at searching for hosts (low a) (Strand, 2000). All non-evolving parameters are fixed and in particular the parasitoids are assumed to have equal attack windows and so Eq. (14) defines the fitness.

In the case of equilibrium underlying population dynamics the singular strategy is defined by the solution, α^* , of

$$\left. \frac{\partial S_P(Q)}{\partial \alpha_q} \right|_{\alpha_q = \alpha_p = \alpha^*} = 0 \Rightarrow f'(\alpha^*) = gHT_{dd}f(\alpha^*). \quad (18)$$

The evolutionary behaviour at the singular strategy can be determined as follows:

$$\text{ES if } \left. \frac{\partial^2 S_P(Q)}{\partial \alpha_q^2} \right|_{\alpha_q = \alpha_p = \alpha^*} < 0 \Rightarrow f''(\alpha^*) - g^2 H^2 T_{dd}^2 f(\alpha^*) < 0. \quad (19)$$

$$\text{CS if } \left. \frac{\partial^2 S_P(Q)}{\partial \alpha_p^2} \right|_{\alpha_q = \alpha_p = \alpha^*} - \left. \frac{\partial^2 S_P(Q)}{\partial \alpha_q^2} \right|_{\alpha_q = \alpha_p = \alpha^*} > 0 \\ \Rightarrow f''(\alpha^*) - gT_{dd}f(\alpha^*)H'(\alpha^*) - g^2 T_{dd}^2 H^2 f(\alpha^*) < 0. \quad (20)$$

It can be shown (see Appendix B) that $H'(\alpha^*) = 0$ in Eq. (20) and so the condition for CS is identical to the condition for ES. Therefore, trade-offs with accelerating costs ($f'' < 0$) and weak decelerating costs ($f'' > 0$ but with low magnitude) are both ES and CS and therefore evolutionary attractors. Trade-offs with strong decelerating costs are neither ES nor CS and are evolutionary repellers. Evolutionary branching cannot occur and therefore the population remains monomorphic.

To verify these results and for continuity with the results for non-equilibrium population dynamics (see later) we undertake multi-strain simulations that approximate the adaptive dynamics process. The simulation methods require that the trade-off function is specified explicitly. We use the following form:

$$a = f(\alpha) = a_{\max} - \frac{(a_{\max} - a_{\min})(\alpha_{\max} - \alpha)}{\alpha_{\max} - \alpha_{\min} + \gamma(\alpha - \alpha_{\min})}, \quad (21)$$

which produces a smooth curve between $(a_{\min}, \alpha_{\min})$ and $(a_{\max}, \alpha_{\max})$ in which the parameter γ controls the curvature (and therefore cost structure) of the trade-off (see Fig. 2). Simulation results are in close agreement with the analytic findings. An evolutionary attractor is shown in Fig. 3A and indicates that strains are attracted towards and fix at the singular strategy.

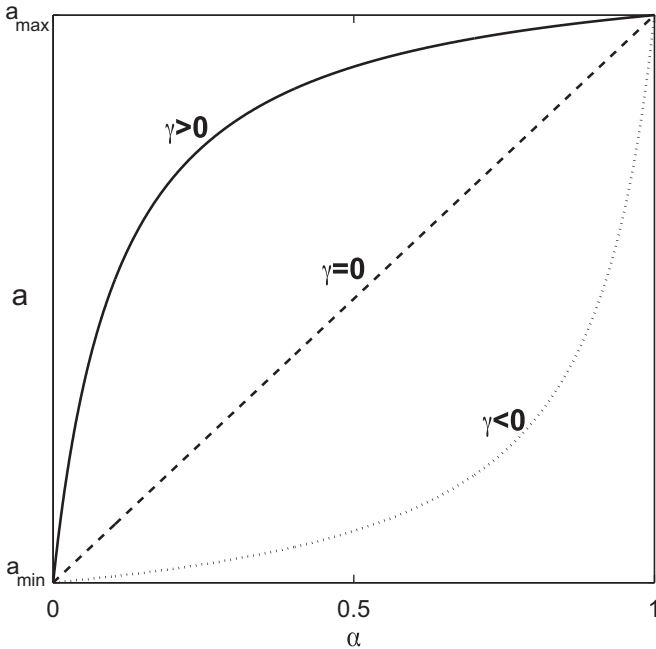


Fig. 2. The trade-off for a versus α . Here $\alpha_{\min} = 0$, $\alpha_{\max} = 1$. The solid line has $\gamma > 0$ and accelerating costs. The dashed line has $\gamma = 0$, and the dotted line has $\gamma < 0$ and decelerating costs.

Strains are repelled away from an evolutionary repeller and reach the minimum (or maximum if the initial value of α is above the singular strategy) attainable value (Fig. 3B). Fig. 3C shows both the position of the singular strategy determined analytically and the final strain of the parasitoid at the end of the evolutionary simulations as a function of the trade-off curvature. The simulations indicate that the population evolves to the singularity for trade-offs with accelerating and weak decelerating costs and evolves away from the singularity for trade-offs with strong decelerating costs (Fig. 3C).

For non-equilibrium underlying population dynamics it is not possible to assess the fitness of the mutant strategy algebraically. Instead we use numerical techniques to compute the fitness functions and produce pairwise invadability plots that indicate the position and nature of the singular strategy. These results are verified using multi-strain simulations. Fig. 3D indicates an evolutionary attractor for accelerating costs and an evolutionary repeller for strong decelerating costs. A singular strategy is not observed in PIPs for trade-offs with weak decelerating costs. Here, the PIPs indicate that the population will evolve to the minimum value of α and this is confirmed by the simulation results.

3.2.2. An α versus t_s trade-off

We consider a trade-off linking parasitoid emergence, α , with the onset of parasitoid attack, t_s , where $\alpha = f(t_s)$. All other parameters are assumed fixed and equal for all parasitoid types. To produce the required trade-off cost structure the benefit of early attack must be associated with the cost of late emergence. Empirical support indicating a relationship between host age and egg-adult development time in koinobiont parasitoids (Harvey, 2005) are consistent with the trade-off being a decreasing function of t_s . When the underlying dynamics are equilibrium the singular strategy occurs when

$$f'(t_s) = - \frac{aP}{gHT_{dd}}.$$

The nature of the singular strategy cannot be determined analytically as the fitness function is not twice differentiable at the singular strategy due to the min/max expressions in t_1 and t_2 . To determine the derivatives of t_1 and t_2 one requires a fixed attack window set-up which is not compatible with this type of trade-off (or any trade-off which involves changing the position of the attack window). Therefore, to determine the nature of the singular point we use numerically generated PIPs and simulation methods.

For equilibrium underlying population dynamics results indicate that trade-offs with strong accelerating costs produce evolutionary attractors, trade-offs with strong decelerating costs produce evolutionary repellers and trade-offs with weak accelerating or decelerating costs lead to evolutionary branching (Fig. 4A). When the underlying population dynamics are non-equilibrium the region of branching is lost and the region where evolutionary repellers occur is extended to all trade-offs with decelerating costs and those with weak accelerating costs (Fig. 4B). The occurrence of branching can be understood by considering a PIP in the region where branching is exhibited (Fig. 4C). It can be seen that the singular strategy is CS but once at the singular strategy parasitoid types with a lower value of α can invade and coexist with the resident type (the fitness is positive directly below the singular strategy). Usually when evolutionary branching occurs the singular strategies can be invaded by types on either side of the singular strategy. The unusual, one-sided invasion properties in this study are a direct result of the discontinuity in the second derivatives of the fitness function at the singular strategy (see Appendix C). Simulations confirm that branching occurs at the singular strategy and two types evolve

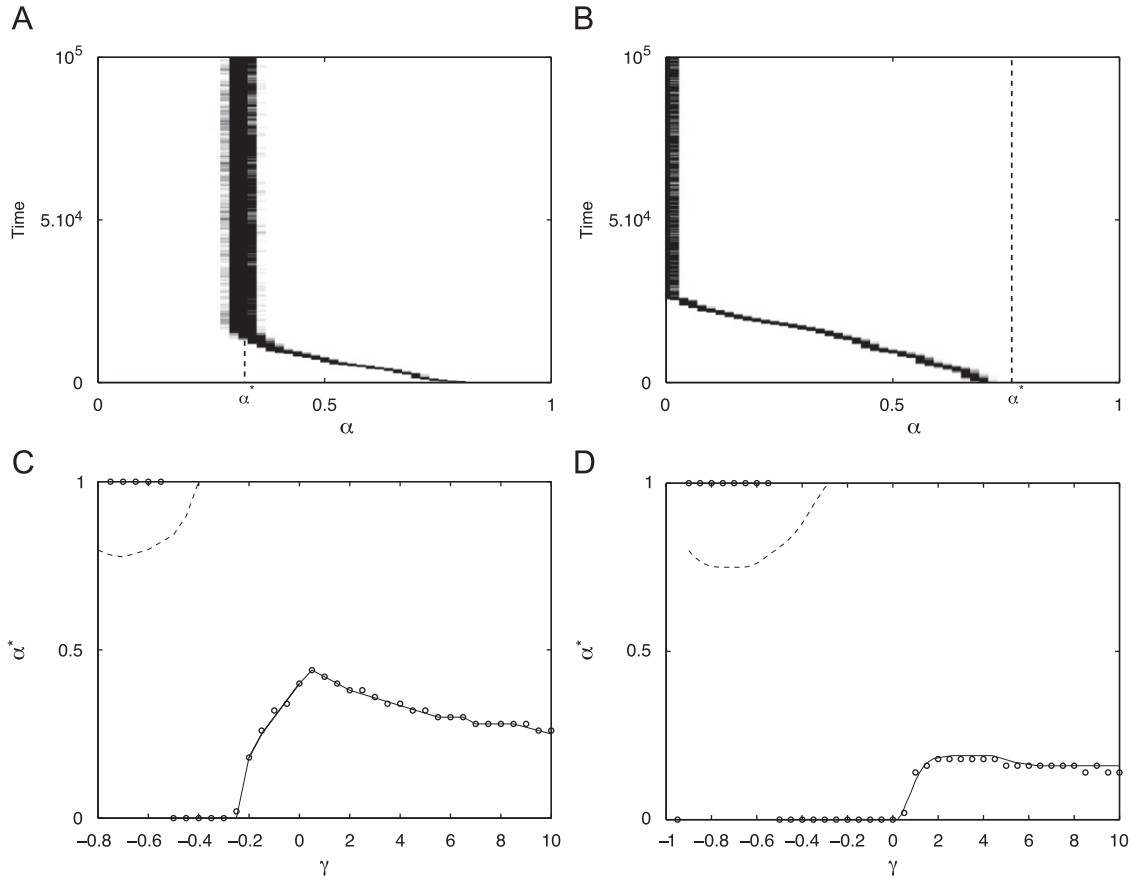


Fig. 3. Simulation results and the position of the singular strategy for an a versus α trade-offs. (A) A single simulation of the evolving value of α showing how the population is attracted to the singular strategy α^* . The underlying dynamics are at equilibrium and the trade-off has accelerating costs, $\gamma = 4$. (B) A single simulation of the evolving value of α showing how the population is repelled away from the singular strategy α^* reaching a final value of α_{min} . The underlying dynamics are at equilibrium and the trade-off has decelerating costs, $\gamma = -0.5$. (C) and (D) the final evolved value of α , represented by circles, and the position of the singular strategy (solid line for attracting and dashed line for repelling singular strategies) for different values of the trade-off curvature, γ . In (C) the underlying population dynamics are at equilibrium. In (D) the underlying dynamics are non-equilibrium. Initially we started each simulation with a monomorphic population in which $\alpha = 0.8$. Parameters are $r=1$, $g=1$, $T_{dd}=0.5$, $T_p = T_q = 0.25$, $t_s=0$, $t_f=0.25$, $\alpha_{min}=0$, $\alpha_{max}=1$ and in (A–C) $a_{min}=3$, $a_{max}=6$ and (D) $a_{min}=15$, $a_{max}=20$.

and coexist with values of α typically lower than that exhibited at the singular point (Fig. 4D).

3.3. The dependence of the singular strategy on other life history parameters

We explore how the position of the singular strategy depends on the length of the host density-dependent period, T_{dd} , the strength of host density-dependence, g , and the length of the parasitoid attack window, $T = T_p = T_q$. We focus on the case where we have a trade-off between a and α . When the underlying population dynamics are at equilibrium we can analytically address this problem. For non-equilibrium dynamics we employ a simulation approach.

Assuming that the underlying dynamics of the system are at a stable equilibrium the dependence of the singular strategy, α^* , on T_{dd} and g , can be found by considering the combined parameter $G = gT_{dd}$ and differentiating Eq. (18). Differentiating both sides of (18) with respect to G , noting that α^* and H are both functions of G , and repeatedly using the chain rule, gives

$$\frac{d\alpha^*}{dG} (f''(\alpha^*) - f(\alpha^*)G^2H^2) = f(\alpha) \left(H + G \frac{dH}{dG} \right) > 0. \quad (22)$$

In Appendix B the Jury conditions are used to show that the sign of the right hand side of (22) is positive. Therefore, the sign of $d\alpha^*/dG$ depends only on the sign of the expression in round brackets, which is precisely Eq. (19) (and therefore (20)), the

condition determining if α^* is ES and CS. When the singular strategy is an evolutionary attractor, $d\alpha^*/dG < 0$ and the value of α^* at the singular strategy decreases as a function of g or T_{dd} . When it is an evolutionary repeller, $d\alpha^*/dG > 0$ and the value of α^* at the singular point increases with g or T_{dd} . An analogous calculation shows that the opposite result holds for dependency of α^* on $T (= t_f - t_s)$, since $dH/dT < 0$.

Simulation methods can be used to confirm the analytical findings and extend the results to the situation where the underlying dynamics are non-equilibrium. In Fig. 5A the evolved value of α is plotted against g . This shows that α^* decreases as g increases for equilibrium dynamics $g > 1.6$, but α^* increases as g increases for non-equilibrium dynamics $g < 1.6$ and there is a clear switch in the trend as the underlying dynamics change from non-equilibrium to equilibrium. Similar findings are observed when the length of the attack window is varied (Fig. 5B). Thus, the trend in the evolved levels of parasitoid parameters depends critically on the nature of the underlying population dynamics.

The behaviour of α^* can be understood biologically for each case as follows. Under equilibrium dynamics (Fig. 5Ai) as g increases, the effect of density-dependence on the parasitoid increases, so the parasitoid evolves to reduce α^* , and thus avoid the ever-strengthening density-dependence, which correlates with parasitoid increased mortality. When the underlying host-parasitoid dynamics are non-equilibrium as g increases the population cycles decrease in amplitude and have smaller average width (compare Fig. 5Aii and iii). This means the impact of host

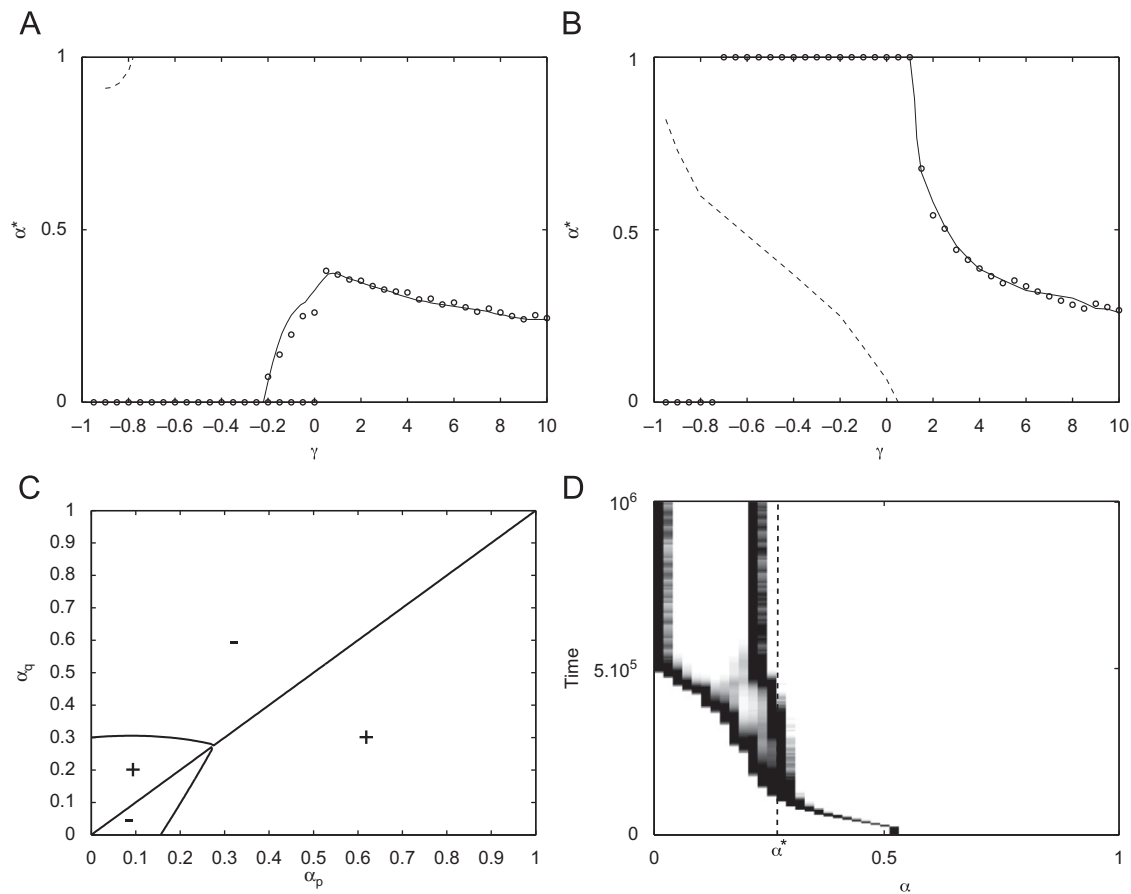


Fig. 4. Simulation results and the position of the singular strategy for an α versus t_s trade-offs. (A) and (B) the final evolved value of α , represented by circles, and the position of the singular strategy (solid line for attracting and dashed line for repelling singular strategies) for different values of the trade-off curvature, γ . In (A) the underlying population dynamics are at equilibrium. Note that for $\gamma \in [-0.25, 2]$ simulations indicate that there is evolutionary branching leading to a dimorphic population (and hence two final evolved values of α). In (B) the underlying dynamics are non-equilibrium and the region of branching is lost. (C) A pairwise invasibility plot (PIP) for $\gamma = -0.1$ in (A). The '+' sign represents where the fitness is positive/negative. The strategies evolve towards the singular point but when close by evolutionary branching occurs as types below the singularity can invade and coexist with the resident. (D) A single simulation of the evolving value of α for the parameters in (C) showing how the population branches. Initially we started each simulation with a monomorphic population in which $\alpha = 0.5$. Parameters are $r=1$, $g=1$, $T_{dd}=0.5$, $T_p=T_q=0.25$, $\alpha_{min}=0$, $\alpha_{max}=1$, t_s $min=0$, t_s $max=0.25$ and in (A), (C) and (D) $a=6$, and (B) $a=15$.

density-dependence reduces and it is more beneficial for the parasitoid to have a larger α and hence a larger attack rate via the trade-off. This is demonstrated in Fig. 5Aiv which indicates that although the average value of host density at the singular strategy, α^* , may decrease, the total density-dependence effect (g multiplied by the average host density) follows the same trend as the evolved value of α^* (Fig. 5A).

As $T (= t_f - t_s)$ increases under equilibrium conditions (Fig. 5Bi), the host density decreases and so the parasitoid can afford to evolve increased α^* . Under non-equilibrium conditions as T increases the cycles have larger amplitude and larger average width (compare Fig. 5Bii and iii) and this leads to an increase in the average host density at the singular strategy and the total density-dependent effect (Fig. 5Biv). Therefore the parasitoid will reduce its α^* in order to lessen the effects of density-dependence.

4. Discussion

We have examined parasitoid evolution in a discrete-time host–parasitoid model using an adaptive dynamics framework. In particular, we have explored the evolution of parasitoid development time and the timing and efficiency of parasitoid attack under equilibrium and non-equilibrium population dynamics. The evolutionary behaviour depends on the shape of the trade-off and

the specific parameters that are linked by the trade-off. For trade-offs with strong accelerating costs we observe evolutionary attractors and for strong decelerating costs non-ES repellers. For these trade-offs the underlying dynamics do not alter the observed evolutionary behaviour but it does alter the boundary, in terms of the trade-off cost structure, that partitions the evolutionary attractor and repeller behaviour. Evolutionary branching is observed for a trade-off between the onset of parasitoid attack and emergence with weak accelerating or decelerating costs. Branching requires that the underlying dynamics exhibit equilibrium behaviour and is lost under non-equilibrium dynamics. The underlying population dynamics are shown to have a striking effect on the value of the evolving life history parameters at the singular strategy with the trend in the evolved parameter switching when the underlying dynamics change from equilibrium to non-equilibrium.

Parasitoids show a wide range of variation in life history properties and this may permit several parasitoids to attack a single host (Godfray et al., 1994; Hawkins, 1994; Memmott et al., 1994). Previous theoretical studies that examine the evolutionary processes that underpin this coexistence have developed host–parasitoid frameworks that include superparasitism or multiparasitism of the host (Bonsall et al., 2004). These mechanisms allow multiple competitors to coexist and parallel the theoretical findings for multi-strain coexistence in more general infectious

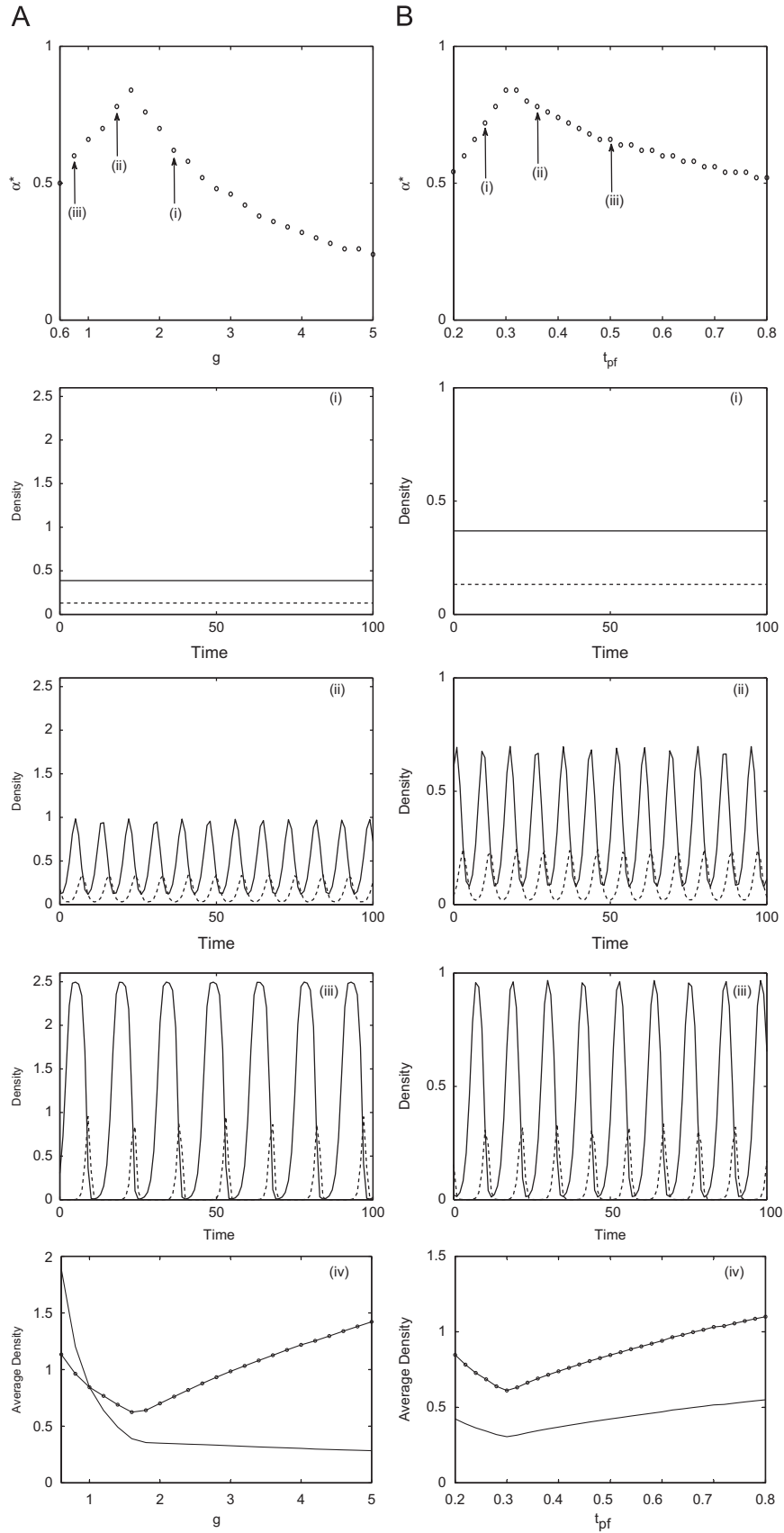


Fig. 5. (A) Final evolved values of α^* for changing strength of host density-dependence, g . (i), (ii), (iii) Dynamics of host-parasitoid system at α^* for various values of g as indicated by the arrows (host: solid line, parasitoid: dashed line). (iv) The average host density over time, H_{av} , (solid line) and the total density-dependence effect, gH_{av} , (solid line with circles) at the evolutionary singular strategy, α^* . (B) Final evolved values of α^* for changing attack window length, t_{pf} . (i), (ii), (iii) Dynamics of host-parasitoid system at α^* for various values of t_{pf} as indicated by the arrows (host: solid line, parasitoid: dashed line). (iv) The average host density over time, H_{av} , (solid line) and the total density-dependence effect, gH_{av} , (solid line with circles) at the evolutionary singular strategy, α^* . All simulations have an a versus α trade-off with $\alpha_{min} = 0$, $\alpha_{max} = 1$, $a_{min} = 10$, $a_{max} = 20$. Initially we started each simulation with a monomorphic population in which $\alpha = 0.5$ and the trade-off curvature is chosen to be $\gamma = 1$, which corresponds to an evolutionary attractor. Other parameters are $T_{dd} = 0.5$, $r = 1$, $t_s = 0$ and in (A) $t_f = 0.25$ and (B) $g = 2$.

disease systems (Nowak and May, 1994). In our study we show how a evolutionary branching can lead to the generation of dimorphic parasitoid strains in a system that does not include super/multiparasitism. Evolutionary branching requires a trade-off between the onset of parasitoid attack and the emergence of the parasitoid from the host. We find that parasitoids that attack early but emerge late from the host can coexist with those that attack later but emerge earlier. Here the benefit to reproduction of early attack is balanced by the cost to mortality of late host emergence. Such evolutionary branching is not specific to a trade-off between onset of parasitoid attack and emergence and can occur when the duration of parasitoid attack is traded-off against emergence or if there is a three way trade-off involving onset of attack, emergence and attack efficiency (see Hackett-Jones et al., 2009). The key criteria is that costs/benefits to reproduction in differences in attack timing are traded-off against mortality effects due to timing in emergence and that the trade-off has a weak cost structure.

Little is known about the effects of development time on parasitoid fitness or the conditions that may select for early emergence at the expense of parasitoid size and future attack efficiency (Harvey, 2005). Early parasitoid attack may provide access to underexploited host populations and early emergence may be an advantage if the host suffers high mortality from other factors. The optimal parasitoid phenotype will depend on trade-offs that link development time to other parasitoid life history properties, which hinges critically on the interaction between growth rate and mortality (Godfray, 1994; Harvey, 2005). Our study indicates that parasitoid development time depends critically on the level of host mortality. Increasing the strength of density-dependence selects to decrease parasitoid emergence/development time under equilibrium dynamics. This is consistent with the findings of Harvey and Strand (2002) who demonstrated that parasitoids exposed to high risks of host mortality exhibit reduced development time in order to minimise this risk. The trend reverses for non-equilibrium dynamics, increasing the strength of density-dependence selects to increase parasitoid emergence/development time. In particular, parasitoids that coexist with hosts that undergo large oscillations with prolonged outbreaks selected for the evolution of early-emergence from the host, while small oscillations in host density led to the evolution of late emerging parasitoids (see Fig. 5). The host oscillations are driven by the host–parasitoid dynamics and large oscillations give rise to an increase in the total host density-dependence effect leading to the selection of early emerging parasitoids to avoid this mortality. When host oscillations are small, the host density-dependence effect is reduced and selection acts to increase parasitoid development time and searching efficiency. Thus, our results are consistent with the general principle that parasitoids facing high mortality risk favour short development times over size and high searching efficiency, whereas species facing low mortality risks favour size at the cost of increased development time (Pennacchio and Strand, 2006). The results are also consistent with Holt et al. (1999) who found that unstable dynamics can weaken or change the direction of selection compared to what is observed under stable equilibrium. The role of non-equilibrium dynamics in parasitoid evolution could be particularly important for insect herbivores and their natural enemies where population cycles are a common occurrence.

Evolutionary branching is observed for certain trade-offs in this study for equilibrium underlying population dynamics. Branching is not observed when the underlying dynamics are non-equilibrium. This contrasts with previous findings for single-species discrete-time models which indicate that evolutionary branching can arise for non-equilibrium underlying population dynamics when it could not occur under equilibrium conditions

(White et al., 2006; Hoyle et al., in press). In White et al. (2006) large population oscillations prevent the maximisation of the birth rate as overcompensating density-dependence acting on the birth rate promotes selection for survival. Our study involves interacting species with density-dependence acting on parasitoid mortality. Under equilibrium conditions there is a benefit to reduced mortality and therefore reduced reproduction and such parasitoids can coexist with those that have higher reproduction but also incur higher mortality. Population oscillations remove the possibility of parasitoid coexistence and therefore must impose additional costs/benefits to mortality and reproduction. This study, therefore, further emphasises the need to understand the role of population oscillation on the evolution of life history properties in ecological systems.

The model presented in this paper clearly demonstrates that the underlying ecological dynamics play an important role in determining the evolution of parasitoid phenology and searching efficiency. A range of empirical relationships between host age attacked and parasitoid egg-to-adult development time and body size have been observed in nature. The feeding ecology of the host is frequently correlated with the evolution of these strategies (Harvey, 2005), as feeding ecology determines host risk to predation and disease. Our work has shown that host mortality from competition can play a similar role in determining the evolution of parasitoid strategies. Our initial attempt to study parasitoid evolution has omitted an explicit description of parasitoid size structure in our model, but rather inferred it from the general observation that high searching efficiency correlates with large adult parasitoids. Parasitoid size is often regarded as an important indicator of fitness and a natural extension of the model with explicit inclusion of host and parasitoid size structure could offer further insights into the range of developmental relationships found empirically. Further studies which examine the host–parasitoid coevolutionary dynamics are needed to fully understand how phenology has evolved in these systems. The evolutionary stability of these phenological relationships in the face of environmental change has implications for population regulation and broader ecological issues such as species invasion.

Acknowledgements

A.W. is supported by a Royal Society of Edinburgh and Scottish Government Support Research Fellowship. We thank Stefan Geritz for the help and advice in the early stages of this research.

Appendix A. Deriving the host–multi-parasitoid model

We outline the derivation of the host–multi-parasitoid model presented in Section 2. A continuous time system of ODEs is used to describe the population dynamics that occur within a season.

The equations for the continuous time model are

$$\frac{dH(t)}{dt} = -a_p H(t)P_0 - a_q H(t)Q_0 - gH_0 H(t), \quad (23)$$

$$\frac{dP(t)}{dt} = a_p H(t)P_0 - gH_0 P(t), \quad (24)$$

$$\frac{dQ(t)}{dt} = a_q H(t)Q_0 - gH_0 Q(t). \quad (25)$$

Here H_0 , P_0 and Q_0 are constants which correspond to the density of hosts and adult parasitoids of type P and Q at the start of the season. Thus, $H(t)$ are the number of host present at time t during the season. Hosts become P or Q parasitised-hosts at rates $a_p P_0$

and $a_q Q_0$ respectively. Both hosts and parasitised-hosts are subjected to density-dependent mortality at rate gH_0 .

The equations above govern the most general situation when both P and Q are attacking the host. For periods where one (or both) of the parasitoids are not attacking the associated searching efficiency is set to zero. Similarly when density-dependence is not operating g is set to zero.

Solving (23) for $H(t)$, and then substituting into the equations for $P(t)$ and $Q(t)$ gives the following general solutions:

$$H(t) = c_1 e^{-(a_p P_0 + a_q Q_0 + gH_0)t}, \quad (26)$$

$$P(t) = -\frac{a_p P_0}{a_p P_0 + a_q Q_0} c_1 e^{-(a_p P_0 + a_q Q_0 + gH_0)t} + c_2 e^{-gH_0 t}, \quad (27)$$

$$Q(t) = -\frac{a_q Q_0}{a_p P_0 + a_q Q_0} c_1 e^{-(a_p P_0 + a_q Q_0 + gH_0)t} + c_3 e^{-gH_0 t}, \quad (28)$$

where c_1, c_2, c_3 are integration constants. To obtain the full discrete-generation equation model we partition the season according to when parasitism by P or Q is occurring (for example see Fig. 1) and use this to find the integration constants and to work out $H(n+1), P(n+1), Q(n+1)$, i.e. the densities at the start of year $n+1$. A full derivation is given in Hackett-Jones et al. (2009).

Appendix B. The nature of the singular strategy when $a = f(\alpha)$

An implicit definition of the coexistence equilibrium is given in (8)–(9). We rewrite it as

$$f(\alpha)TP = r - gT_{dd}H = f(\alpha)THE^{-\alpha gT_{dd}H}(1 - e^{-r + gHT_{dd}}) \quad (29)$$

which is biologically realistic provided $gT_{dd}H < r$. A trade-off has been introduced such that $a_p = f(\alpha)$. To simplify the notation we introduce $F(\alpha) = Tf(\alpha)$ and $G = gT_{dd}$.

Claim B.1. $dH/d\alpha = 0$ at the singular strategy, $\alpha = \alpha^*$.

Proof. We differentiate Eq. (29) with respect to α and collect terms as follows:

$$\frac{dH}{d\alpha} \overbrace{\left(G + (F(\alpha)e^{-\alpha GH} - G\alpha F(\alpha)He^{-\alpha GH})(1 - e^{-r + GH}) - GF(\alpha)He^{-\alpha GH}e^{-r + GH} \right)}^{\Psi} = F(\alpha)He^{-\alpha GH}GH(1 - e^{-r + GH}) - HF'(\alpha)e^{-\alpha GH}(1 - e^{-r + GH}). \quad (30)$$

Using Eq. (29) we obtain

$$\Psi = G + \frac{r - GH}{H} + G(r - GH)(1 - \alpha) - GF(\alpha)He^{-\alpha GH} = \frac{1 - \text{tr } \mathbf{J} + \det \mathbf{J}}{H} > 0, \quad (31)$$

where \mathbf{J} is the Jacobian associated to the coexistence steady state. Since we are assuming (H, P) is a stable steady state the three Jury conditions must be satisfied (Jury, 1964, 1974). Therefore $1 - \text{tr } \mathbf{J} + \det \mathbf{J} > 0$ and hence $\Psi > 0$.

The condition for a CS (20) requires evaluating $dH/d\alpha$ at the singular strategy α^* . At α^* , $F'(\alpha^*) = GHF(\alpha^*)$ substituting this into the RHS of (30) gives

$$\frac{dH}{d\alpha} \Psi = 0 \Rightarrow \frac{dH}{d\alpha} = 0. \quad \square$$

This result is a consequence of the trade-off between α and a_p . Independently, a and α have opposing effects on the coexistence steady state. H is an increasing function of α (shown analytically here by setting $f'(\alpha) = 0$), and decreases as a function of a .

Claim B.2. $H + G(dH/dG) > 0$ at the singular strategy $\alpha = \alpha^*$.

Proof. We follow the method of Claim B.1 and differentiate Eq. (29) with respect to G and collect terms as follows:

$$\frac{dH}{dG} \overbrace{\left(\frac{r}{H} + G(r - GH)(1 - \alpha) - GF(\alpha)He^{-\alpha GH} \right)}^{\Psi} = -H + F(\alpha)He^{-\alpha GH}\alpha H(1 - e^{-r + GH}). \quad (32)$$

First notice that on the LHS of (32) we have Ψ which we proved was positive in Claim B.1. The RHS of (32) can be rewritten as follows:

$$-H - H(1 - \alpha)(r - GH) + F(\alpha)H^2 e^{-\alpha GH} = -H - \left(\frac{1 - \text{tr } \mathbf{J} + \det \mathbf{J}}{G} \right) + \frac{r}{G}. \quad (33)$$

Thus, by (33) and (31)

$$H + G \frac{dH}{dG} = \frac{H(r - GH)}{1 - \text{tr } \mathbf{J} + \det \mathbf{J}} > 0$$

by the Jury (1964, 1974) conditions as required. \square

Appendix C. Continuity of derivatives of the fitness expression at the singular strategy

In this section we consider the trade-off $\alpha = f(t_{qs})$. The first and second partial derivative of the fitness expression $s_P(Q)$ (given by Eqs. (10) and (11)) with respect to t_{qs} evaluated at the singular strategy are given by

$$\frac{\partial s_P(Q)}{\partial t_{qs}} = \frac{1}{\Phi} \left[-gHT_{dd}\Phi f' + \frac{\partial \Phi}{\partial t_{qs}} \right]_* \quad (34)$$

$$\frac{\partial^2 s_P(Q)}{\partial t_{qs}^2} \Big|_* = \frac{1}{\Phi} \left[(gHT_{dd})^2 \Phi (f')^2 - \Phi gHT_{dd} f'' - 2 \frac{\partial \Phi}{\partial t_{qs}} gHT_{dd} f' + \frac{\partial^2 \Phi}{\partial t_{qs}^2} \right]_* \quad (35)$$

respectively, where f' denotes derivative with respect to t_{qs} and $*$ denotes evaluation at the singular strategy $t_{qs} = t_{ps} = t_{qs}^*$. At the singular strategy it is easy to show $\Phi = 1$. However, the derivatives terms, $\partial \Phi / \partial t_{qs}$ and $\partial^2 \Phi / \partial t_{qs}^2$ are more complicated as the involve derivatives of t_1 etc., with respect to t_{qs} . These functions involve minimum and maximum expressions whose values depend on whether $t_{qs} > t_{ps}$ and $t_{ps} > t_{qs}$. In the case of $\partial \Phi / \partial t_{qs}$,

$$\frac{\partial \Phi}{\partial t_{qs}} = \frac{aP}{(1 - e^{-aPT})} \left(\frac{\partial}{\partial t_{qs}} (t_{p(a)} - t_{q(a)}) + e^{-aPT} \frac{\partial}{\partial t_{qs}} (t_1 - t_{p(a)} + t_{qf} - t_{q(b)}) \right)$$

and the derivatives on the right hand side take the same values in both the case of $t_{qs} > t_{ps}$ and $t_{ps} > t_{qs}$ giving $\partial \Phi / \partial t_{qs}|_* = -aP$. Hence the first derivative of the fitness expression is continuous. This is not the case for the second derivative. The derivatives involving t_1 etc., in Eq. (35) do depend on whether $t_{qs} > t_{ps}$ giving rise to a discontinuity in this derivative,

$$\frac{\partial^2 \Phi}{\partial t_{qs}^2} \Big|_* = \begin{cases} \frac{-a^2 P^2 e^{-aPT}}{1 - e^{-aPT}} & \text{if } t_{ps} > t_{qs}, \\ a^2 P^2 & \text{if } t_{ps} < t_{qs}. \end{cases}$$

Consequently, $\partial^2 s_P(Q) / \partial t_{qs}^2|_*$ is also discontinuous. The continuous first derivative of the fitness expression allows us to analytically find the singular strategy, the discontinuity in the second derivative prevents us from analytically determining the nature of the evolutionary singular strategy.

References

Beddington, J.R., Free, C.A., Lawton, J.H., 1975. Dynamic complexity in predator-prey models framed in difference equations. *Nature* 255, 58–60.

- Berryman, A.A., 1996. What cause population cycles of forest Lepidoptera? *TREE* 11 (1), 28–32.
- Best, A., White, A., Boots, M., 2009. The implications of coevolutionary dynamics to host–parasite interactions. *Am. Nat.* 173, 779–791.
- Best, A., White, A., Kisdi, E., Antonovics, J., Brockhurst, M., Boots, M., 2010. Evolution of host–parasite range. *Am. Nat.* 176, 63–71.
- Bonsall, M.B., Jansen, V.A.A., Hassell, M.P., 2004. Life history trade-offs assemble ecological guilds. *Science* 306, 111–114.
- Cobbold, C.A., Roland, J., Lewis, M.A., 2009. The impact parasitoid emergence time on host–parasitoid population dynamics. *Theor. Popul. Biol.* 75, 201–215.
- Dieckmann, U., Metz, J.A.J., Sabelis, M.W., Sigmund, K. (Eds.), 2002. *Adaptive Dynamics of Infectious Diseases: in Pursuit of Virulence Management*. Cambridge University Press, Cambridge.
- Eckmann, J.-P., Ruelle, D., 1985. Ergodic theory of chaos and strange attractors. *Rev. Mod. Phys.* 57, 617–656.
- Fellowes, M.D.E., Travis, J.M.J., 2000. Linking the coevolutionary and population dynamics of host–parasitoid interactions. *Popul. Ecol.* 42 (2), 195–203.
- Ferriere, R., Gatto, M., 1993. Chaotic population dynamics can result from natural selection. *Proc. R. Soc. B* 251, 33–38.
- Geritz, S.A.H., Kisdi, E., Meszner, G., Metz, J.A.J., 1998. Evolutionary singular strategies and the adaptive growth and branching of the evolutionary tree. *Evol. Ecol.* 12, 35–57.
- Godfray, H.C.J., Waage, J.K., 1991. Predictive modeling in biological control: the mango mealybug (*Rastrococcus invadens*) and its parasitoids. *J. Appl. Ecol.* 28, 434–453.
- Godfray, H.C.J., 1994. *Parasitoids, Behavioural and Evolutionary Biology*. Princeton University Press, Princeton.
- Godfray, H.C.J., Hassell, M.P., Holt, R.D., 1994. The population dynamic consequences of phenological asynchrony between parasitoids and their hosts. *J. Anim. Ecol.* 63, 1–10.
- Gandon, S., Rivero, A., Varaldi, J., 2006. Superparasitism evolution: adaptation or manipulation? *Am. Nat.* 167 (1), E1–E22.
- Hackett-Jones, E., Cobbold, C.A., White, A., 2009. Coexistence of multiple parasitoids on a single host due to differences in parasitoid phenology. *Theor. Ecol.* 2 (1), 19–31.
- Harvey, J.A., 2005. Factors affecting the evolution of development strategies in parasitoid wasps: the importance of functional constraints and incorporating complexity. *Entomol. Exp. Appl.* 117, 1–13.
- Harvey, J.A., Strand, M.R., 2002. The developmental strategies of endoparasitoid wasps vary with host feeding ecology. *Ecology* 83 (9), 2439–2451.
- Hawkins, B.A., 1994. *Pattern and Process in Host–Parasitoid Interactions*. Cambridge University Press, Cambridge.
- Holt, R.D., Hochberg, M.E., Barfield, M., 1999. Population dynamics and the evolutionary stability of biological control. In: Hawkins, B., Cornell, H. (Eds.), *Theoretical Approaches to Biological Control*. Academic Press, New York, pp. 219–230.
- Hoyle, A., Bowers, R.G., White, A., in press. Evolutionary Behaviour trade-offs and cyclic and chaotic population dynamics. *Bull. Math. Biol.*, doi:10.1007/s11538-010-9567-7.
- Jury, E.I., 1964. *Theory and Application of the Z-Transform method*. Wiley New York.
- Jury, E.I., 1974. *Inners and Stability of Dynamical Systems*. Wiley, New York.
- Kon, R., Takeuchi, Y., 2001. The effect of evolution on host–parasitoid systems. *J. Theor. Biol.* 209, 287–302.
- McGregor, R.R., Roitberg, B.D., 2000. Size-selective oviposition by parasitoids and the evolution of life-history timing by hosts: fixed preferences vs frequency-dependent host selection. *OIKOS* 89, 305–312.
- Memmott, J., Godfray, H.C.J., Gault, I.D., 1994. The structure of a tropical host parasitoid community. *J. Anim. Ecol.* 63 (3), 521–540.
- Metz, J.A.J., Nesbit, R.M., Geritz, S.A.H., 1992. How should we define “fitness” for general ecological scenarios? *TREE* 7, 198–202.
- Metz, J.A.J., Geritz, S.A.H., Meszner, G., Jacobs, F.J.A., Van Heerwaarden, J.S., 1996. Adaptive dynamics: a geometrical study of the consequences of nearly faithful reproduction. In: Van Strien, S.J., Verduyn Lunel, S.M. (Eds.), *Stochastic and Spatial Structures of Dynamical Systems*. Elsevier, pp. 183–231.
- Nicholson, A.J., Bailey, V.A., 1935. The balance of animal populations part 1. *Proc. Zool. Soc. London* 3, 551–598.
- Nowak, M., 1990. An evolutionarily stable strategy may be inaccessible. *J. Theor. Biol.* 142, 237–241.
- Nowak, M.A., May, R.M., 1994. Superinfection and the evolution of parasite virulence. *Proc. R. Soc. B* 255, 81–89.
- Parry, D., 1994. The impact of predators and parasitoids on natural and experimentally created populations of forest tent caterpillar. *Malacosoma disstria* Hubner (Lepidoptera: Lasiocampidae). Master’s Thesis. University of Alberta, Edmonton, Alberta.
- Pennacchio, F., Strand, M.R., 2006. Evolution of developmental strategies in parasitic hymenoptera. *Annu. Rev. Entomol.* 52, 233–258.
- Pugliese, A., 2002. On the evolutionary coexistence of parasite strains. *Math. Biosci.* 177–178, 355–375.
- Ringel, M.S., Rees, M., Godfray, H.C.J., 1998. The evolution of diapause in a coupled host–parasitoid system. *J. Theor. Biol.* 194, 195–204.
- Sasaki, A., Godfray, H.C.J., 1999. A model for the coevolution of resistance and virulence in coupled host–parasitoid interactions. *Proc. R. Soc. B* 266, 455–463.
- Sisterson, M.S., Averill, A.L., 2004. Coevolution across landscapes: a spatially explicit model of parasitoid–host coevolution. *Evol. Ecol.* 18, 29–49.
- Strand, M.R., 2000. Developmental traits and life-history evolution in parasitoids. In: Hochberg, M.E., Ives, A.R. (Eds.), *Parasitoid Population Biology*. Princeton University Press, Princeton, pp. 139–162.
- Visser, M.E., Both, C., 2005. Shifts in phenology due to global climate change: the need for a yardstick. *Proc. R. Soc. B* 272, 2561–2569.
- Wang, Y.H., Gutierrez, A.P., 1980. An assessment of the use of stability analyses in population ecology. *J. Anim. Ecol.* 49, 435–452.
- White, A., Greenman, J.V., Benton, T.G., Boots, M., 2006. Evolutionary behaviour in ecological systems with trade-offs and non-equilibrium population dynamics. *Evol. Ecol. Res.* 8, 387–398.